

Report No. BMI-1333
UC-25 Metallurgy and Ceramics
(TID-4500, 14th Ed.)

Contract No. W-7405-eng-92

IRRADIATION OF CLAD GRAPHITE IN HIGH-TEMPERATURE
HIGH-PRESSURE CO₂

by

John C. Smith
William E. Murr
Ward S. Diethorn
William H. Goldthwaite

April 7, 1959

BATTELLE MEMORIAL INSTITUTE
505 King Avenue
Columbus 1, Ohio

DISCLAIMER

This report was prepared as an account of work sponsored by an agency of the United States Government. Neither the United States Government nor any agency Thereof, nor any of their employees, makes any warranty, express or implied, or assumes any legal liability or responsibility for the accuracy, completeness, or usefulness of any information, apparatus, product, or process disclosed, or represents that its use would not infringe privately owned rights. Reference herein to any specific commercial product, process, or service by trade name, trademark, manufacturer, or otherwise does not necessarily constitute or imply its endorsement, recommendation, or favoring by the United States Government or any agency thereof. The views and opinions of authors expressed herein do not necessarily state or reflect those of the United States Government or any agency thereof.

DISCLAIMER

Portions of this document may be illegible in electronic image products. Images are produced from the best available original document.

TABLE OF CONTENTS

	<u>Page</u>
ABSTRACT	1
INTRODUCTION	1
BACKGROUND	1
EXPERIMENTAL PROGRAM	2
Plan of Experiment	2
Specimens	3
Irradiation Environment	3
Methods of Evaluation	3
Preparation of Irradiation Capsule and Associated Equipment	6
Design and Construction of Capsule	6
Out-of-Pile Tests of Capsule	12
Design of Associated Equipment	12
Irradiation History	13
Postirradiation Examination Techniques	13
Physical Measurements	15
Metallography	15
Results of Postirradiation Examination	15
Visual Examination	15
Physical Measurements	19
Metallographic Examination	19
Inconel	25
Type 310 Stainless Steel	25
Type 446 Stainless Steel	25
CONCLUSIONS	26
REFERENCES	26

IRRADIATION OF CLAD GRAPHITE IN HIGH-TEMPERATURE HIGH-PRESSURE CO₂

John C. Smith, William E. Murr, Ward S. Diethorn,
and William H. Goldthwaite

Graphite specimens fully clad with Type 310 stainless, Type 446 stainless or Inconel were irradiated in a 1000-psi carbon dioxide environment for a period of 4 weeks at approximately 1300 F followed by 1 week at 1500 F. The fast-neutron-plus-gamma dose rate was estimated at 8×10^7 rads per hr. The gas environment was sampled and replenished eight times during the experiment. After 60 hr at about 1350 F, the carbon monoxide content had increased from a negligible value to 3.6 volume per cent. It then decreased steadily to a value of 0.4 volume per cent at the end of 4 weeks. When the temperature was raised to 1500 F, the CO content increased to 1.9 volume per cent in 100 hr and then decreased to 0.6 volume per cent. The oxygen content remained nearly constant throughout the experiment. Postirradiation examination and metallography revealed very little effect of the exposure on the cladding materials at the gas and graphite interfaces.

INTRODUCTION

As part of the core-materials evaluation for the Maritime Gas-Cooled Reactor, General Atomic is investigating high-temperature corrosion in a candidate moderator-coolant system consisting of fully clad graphite and high-pressure CO₂. In support of General Atomic's program Battelle has conducted a one-capsule irradiation study of this system in the BRR. Graphite specimens fully clad with Type 310 or Type 446 stainless steel or with Inconel were irradiated for 5 weeks in high-pressure high-temperature CO₂. Samples of the gas were removed from the capsule during the experiment and analyzed for CO and oxygen. The postirradiation examination of the specimens included dimensional, weight, and density measurements, metallography, and microhardness determinations.

This report summarizes the design and results of the experiment.

BACKGROUND

One of the problems in a graphite-moderated and CO₂-cooled high-temperature reactor is corrosion of the metallic core materials. If corrosion of the cladding exposes the graphite moderator to the CO₂ coolant, carbon transport via the CO₂-CO-graphite equilibrium is expected to be serious. Both thermodynamic considerations and the corrosion literature suggest that candidate metals are attacked at temperatures as low as 1500 F. At lower temperatures the 18:8 stainless steels show good corrosion resistance, the British reporting⁽¹⁾ negligible attack after 5-month exposures in static CO₂ at 8 atm and 1000 F.

(1) References at end.

Three processes in the reactor will contribute small amounts of CO and oxygen to the CO₂ coolant:

- (1) Radiolysis of the CO₂, producing CO and oxygen
- (2) Thermal reaction between metals and CO₂, giving metal oxides and CO
- (3) The chemical equilibrium $2\text{CO}_2 \rightleftharpoons 2\text{CO} + \text{O}_2$.

The corrosion is influenced by the CO and oxygen, and it is clear that temperature, pressure, and radiation affect the concentrations of these coolant components. In the absence of radiation, the concentrations of CO and oxygen in chemical equilibrium with CO₂ are extremely low at 1500 F. Radiation may possibly support higher CO and oxygen concentrations than those characteristic of the chemical equilibrium. In a radiation field at temperatures of 200 F, for example, the CO and oxygen concentrations are higher than the chemical-equilibrium values and increase with CO₂ pressure.⁽²⁾ The concentrations are sensitive to impurities in the CO₂. No irradiation data are available on high-temperature and high-pressure CO₂. However, in-pile-loop studies of the CO₂-graphite system in BEPO provided some relevant information.⁽³⁾ A steady-state concentration of 0.2 to 0.5 volume per cent CO was reached in the CO₂ after a few reactor cycles. Temperature and pressure conditions were not specified, but presumably they were about 700 F and 10 atm, characteristic of Calder Hall coolant conditions.

Carbide formation at the graphite-cladding interface is also a potential problem at high temperatures because of the effect of carbide on cladding strength and integrity. Carbon dioxide may influence this reaction in a local cladding failure, but if the cladding does not fail and graphite is not exposed to the gas, carbide formation at the interface should be independent of the CO₂ environment. Carbide formation is not expected to be sensitive to radiation. However, no high-temperature irradiation data are available to support this conclusion.

An extrapolation of these fragmentary data to the capsule experiment is difficult. There is evidence for two generalizations, however. The effects of temperature and radiation on the composition of the CO₂ coolant, and hence the corrosion of metals, are not independent. Secondly, of two effects, temperature should dominate the corrosion if the CO₂-CO-O₂ chemical equilibrium is reached rapidly.

EXPERIMENTAL PROGRAM

Plan of Experiment

The objective of this experiment was to obtain information about the effects of irradiation on the corrosion of potential cladding materials for graphite that are exposed to a high-temperature high-pressure CO₂ environment. Since carburization of cladding materials in intimate contact with the graphite moderator is a potential problem at high temperatures, the effects of radiation on this reaction were also of interest. These effects were studied by a 6-week irradiation of small graphite cylinders tightly clad

with selected materials in a capsule containing CO_2 at high temperature and pressure. The total gamma-and-fast-neutron dose rate was estimated to be 8×10^7 rads per hr. To isolate the effects of irradiation from strictly thermal effects, a duplicate test was conducted out-of-pile at General Atomic.

Specimens

The specimens that were studied consisted of 1 by 1-cm cylinders of AGOT graphite clad with Types 310 or 446 stainless steel or with Inconel. Two specimens clad with each of the three materials were irradiated. A third specimen of each type was examined as a control. The specimens were fabricated at General Atomic. In the assembly operation, a graphite cylinder was placed into a 30-mil-wall tube of the cladding material; machined end plugs, 60 mils thick, were welded in air to the tube ends, and then the tube was swaged. The specimens are pictured in Figures 1 and 2.

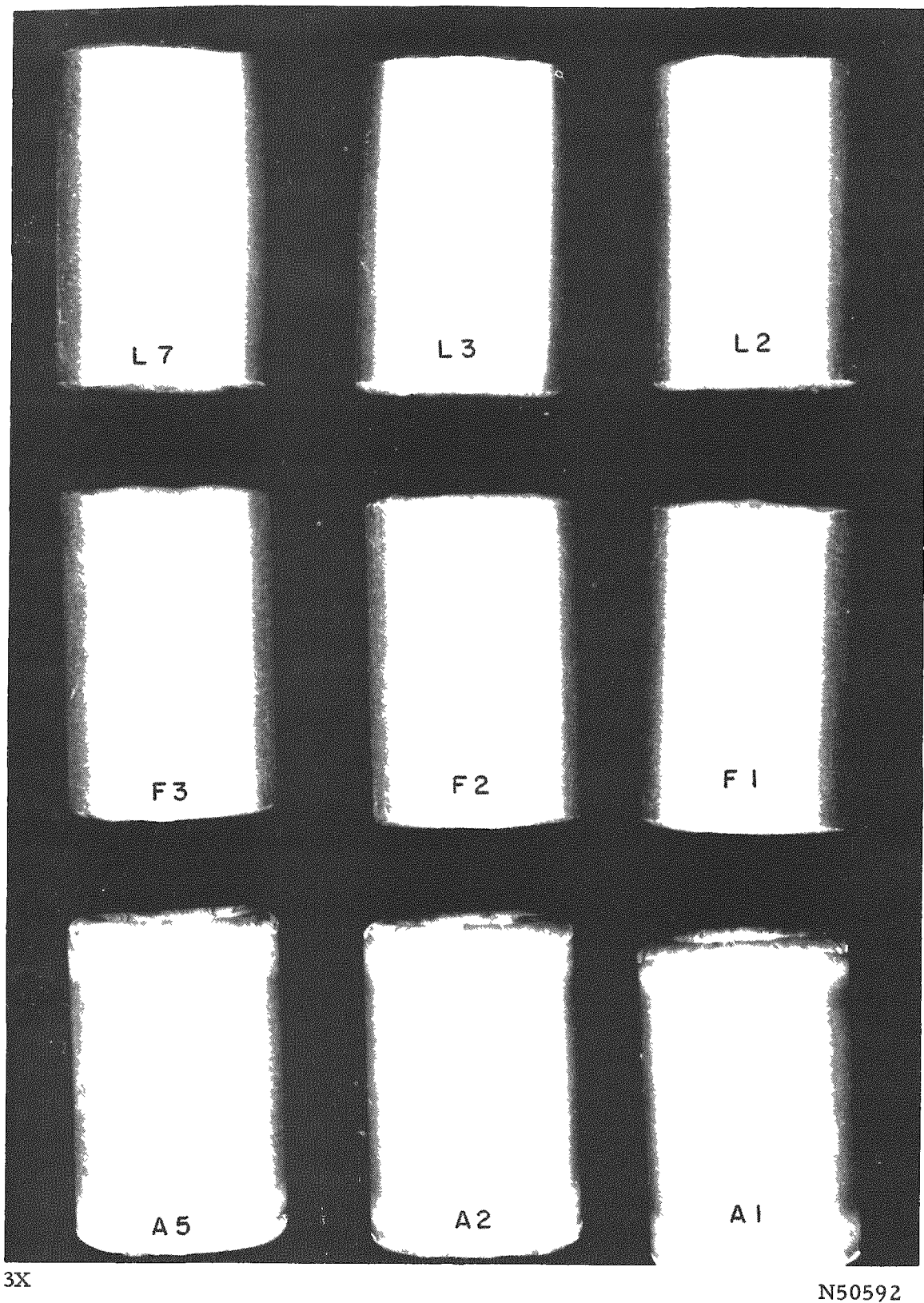
Irradiation Environment

Although the maximum CO_2 prototype reactor coolant temperatures and pressures had not been fixed at the time of this experiment, there was sufficient interest in temperatures up to 1500 F and pressures up to 2000 psi to plan the experiment around these values. It was felt that a 1500 F CO_2 environment could be obtained without great difficulty. However, since CO_2 is supplied in tanks at 870 psi, special techniques would have had to be used to provide a 2000-psi CO_2 atmosphere. A pressure of 1000 psi appeared to be feasible and was obtained by pressurizing the cold capsule to 750 psi and allowing the temperature to rise to 1500 F to increase the pressure to 1000 psi.

Originally, it was felt that changes in the composition of the gas during the exposure would provide information on the reactions that were occurring at the cladding surface. As it developed, these reactions were probably overshadowed by reactions with the extended high-temperature surfaces of the capsule itself. Nevertheless, gas samples were taken and fresh gas was introduced several times during the irradiation to avoid depletion as much as possible of any of the constituents of the gas mixture by reactions with the capsule or specimen surfaces.

Methods of Evaluation

Measurements of the specimen dimensions, weights, and densities before and after irradiation were made to reveal any gross damage or corrosion of the specimens. Metallographic examinations and microhardness measurements of control and irradiated specimens were made to study less obvious changes in the cladding materials as a result of the exposure.

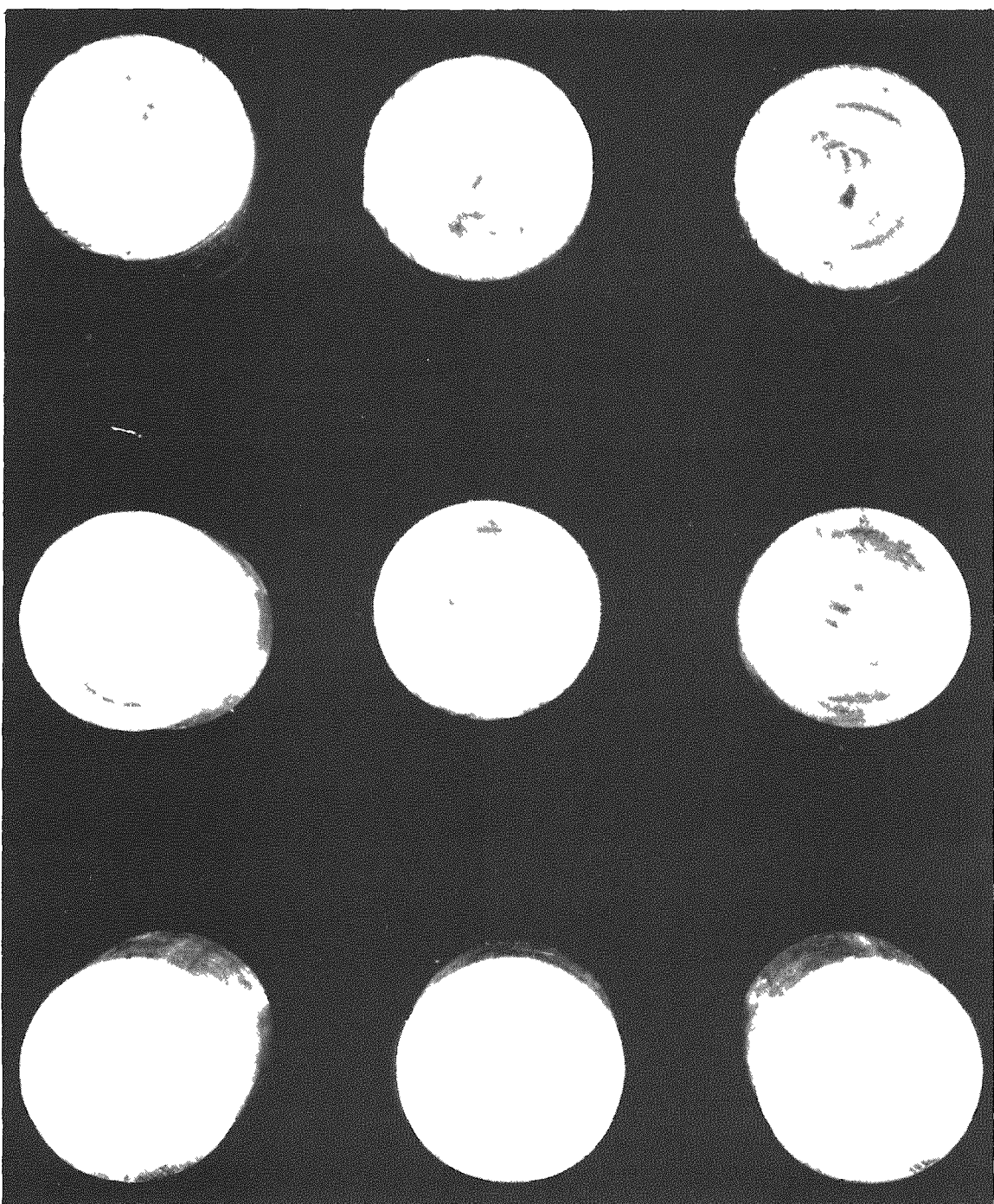


3X

N50592

FIGURE 1. SIDE VIEW OF CLAD-GRAFITE SPECIMENS

Specimen cladding materials: top row, Inconel;
middle row, Type 446 stainless steel; bottom
row, Type 310 stainless steel.



N50594

FIGURE 2. END VIEW OF CLAD-GRAphITE SPECIMENS

Specimen cladding materials: top row, Type 310 stainless steel; middle row, Type 446 stainless steel; bottom row, Inconel.

Preparation of Irradiation Capsule and Associated Equipment

Design and Construction of Capsule

The principal factors which governed the design of the irradiation capsule were:

- (1) Specimen size (0.44 in. in diameter by 0.7 in. long)
- (2) Environment (CO₂ at 1500 F and 1000 psi)
- (3) Dimensions of irradiation facility (3 by 3-in. BRR core-lattice position)
- (4) Desirability of sampling and replenishing the gas during the irradiation
- (5) Capsule-materials compatibility with CO₂
- (6) Amenability to hot-cell handling and opening techniques
- (7) Reliability
- (8) Safety
- (9) Schedule.

As originally scheduled, the irradiation was to begin only 6 weeks after the initiation of the research. With so little time available, the design had to be straightforward and such that existing fabrication techniques could be used for construction and assembly.

As can be seen in Figures 3, 4, and 5, the capsule was basically an outer pressure shell, 1-3/4 in. in diameter, cooled to about 100 F by the reactor coolant water, and an inner furnace tube. The specimens were positioned within the furnace tube by the crosspieces of a basket made of 1/16-in.-diameter Type 310 stainless wire.

The furnace tube was fabricated by brazing Type 304 stainless steel-sheathed MgO-insulated Kanthal electric heaters, 1/16 in. in diameter, to the outside surface of a thin-walled Type 304 stainless tube. The heaters, each nominally rated at 1000 w, contain a 50-in. length of 0.018-in.-diameter Kanthal high-resistance wire with 12-in. low-resistance nickel leads of the same diameter butt welded to the ends of the Kanthal. By having the entire heater, including the nickel leads, within the sheath only the low-resistance low-power nickel lead region of the heater need be in the space between the top of the furnace tube and the end cap. In this region, the heat must be dissipated from the small area of the sheath rather than from the extended area of the furnace tube. The heater sheath extended through and was brazed to the end cap. Beyond the end cap, the sheath was stripped so that the nickel lead could be connected at the Lavite terminal block to copper leads from the external heater power supply.

The heater was furnace brazed to the furnace tube using GE-81 brazing alloy, which has a remelt temperature of about 2150 F. The brazing operation requires the application of a precise amount of braze to provide a fillet between the heater and

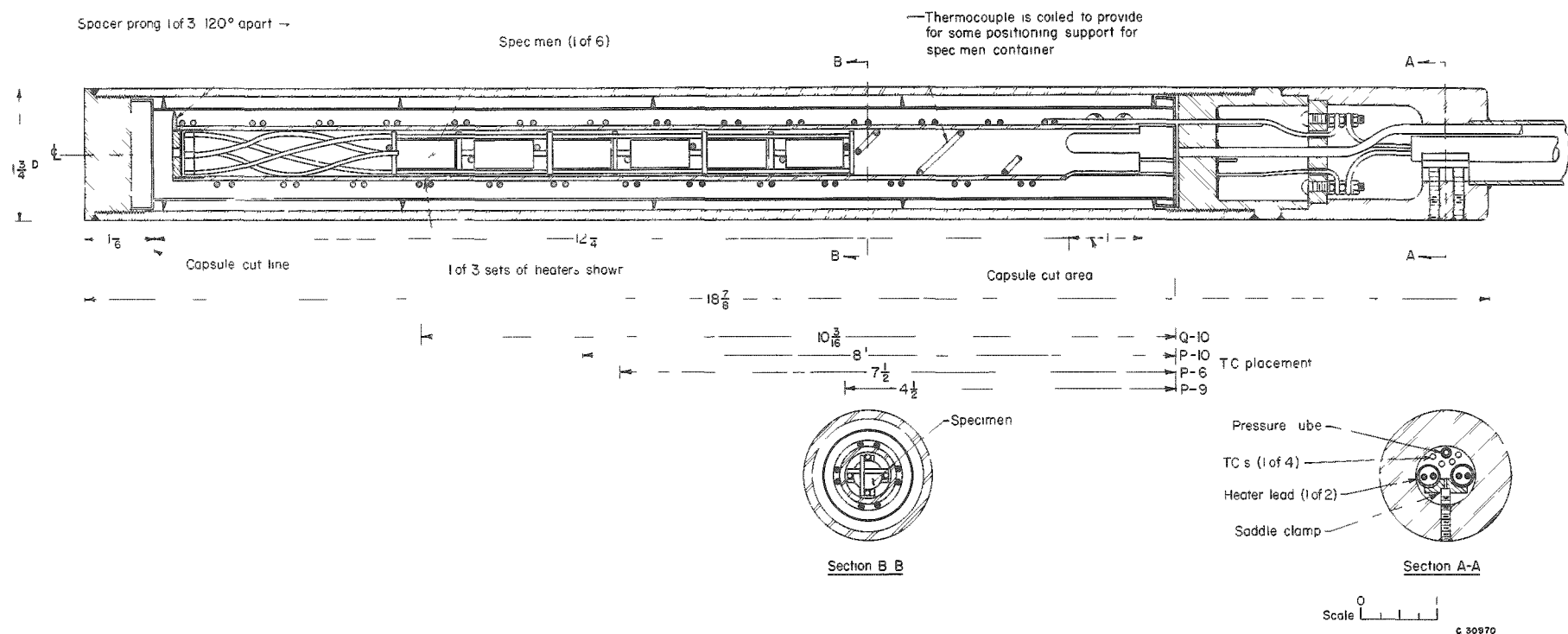
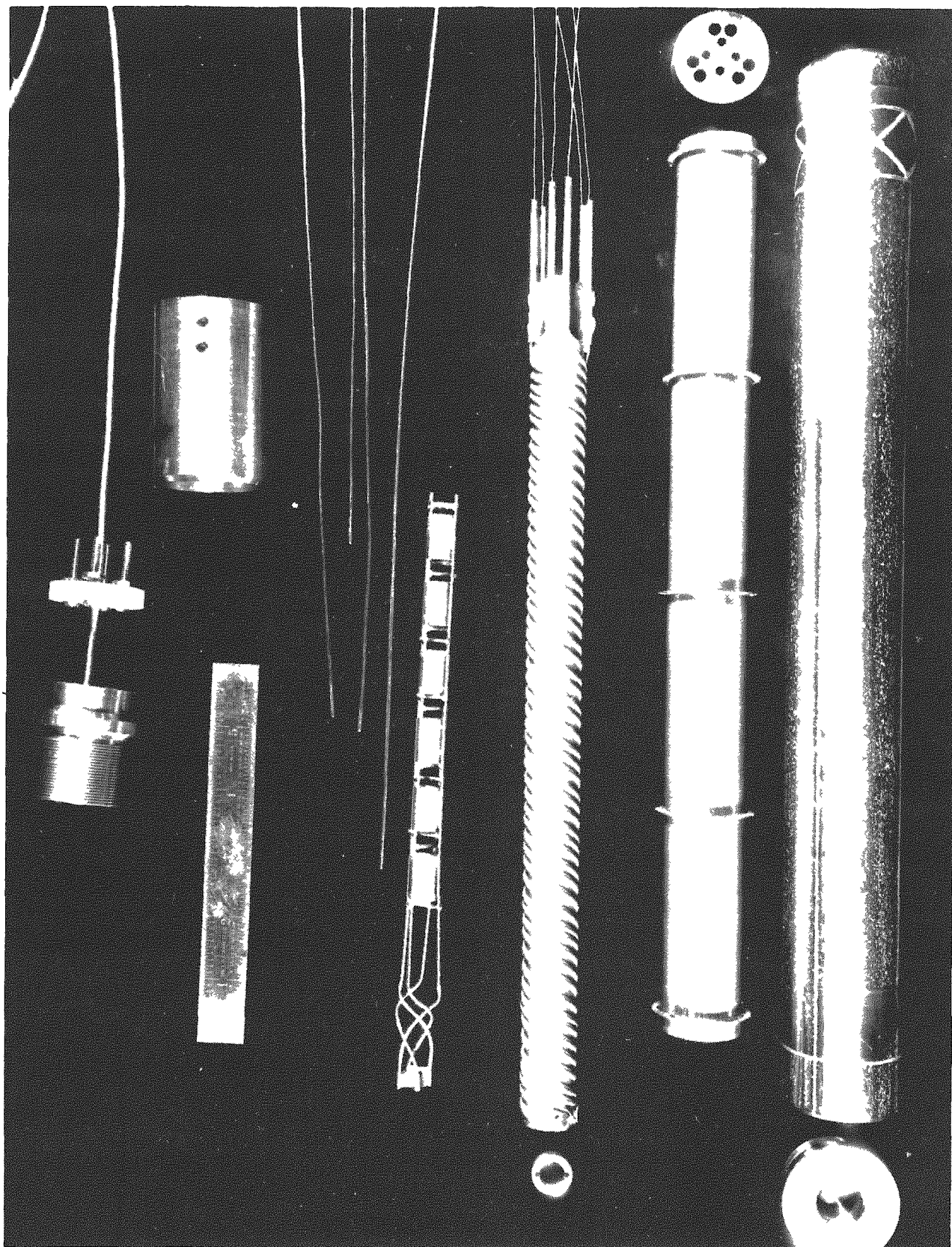
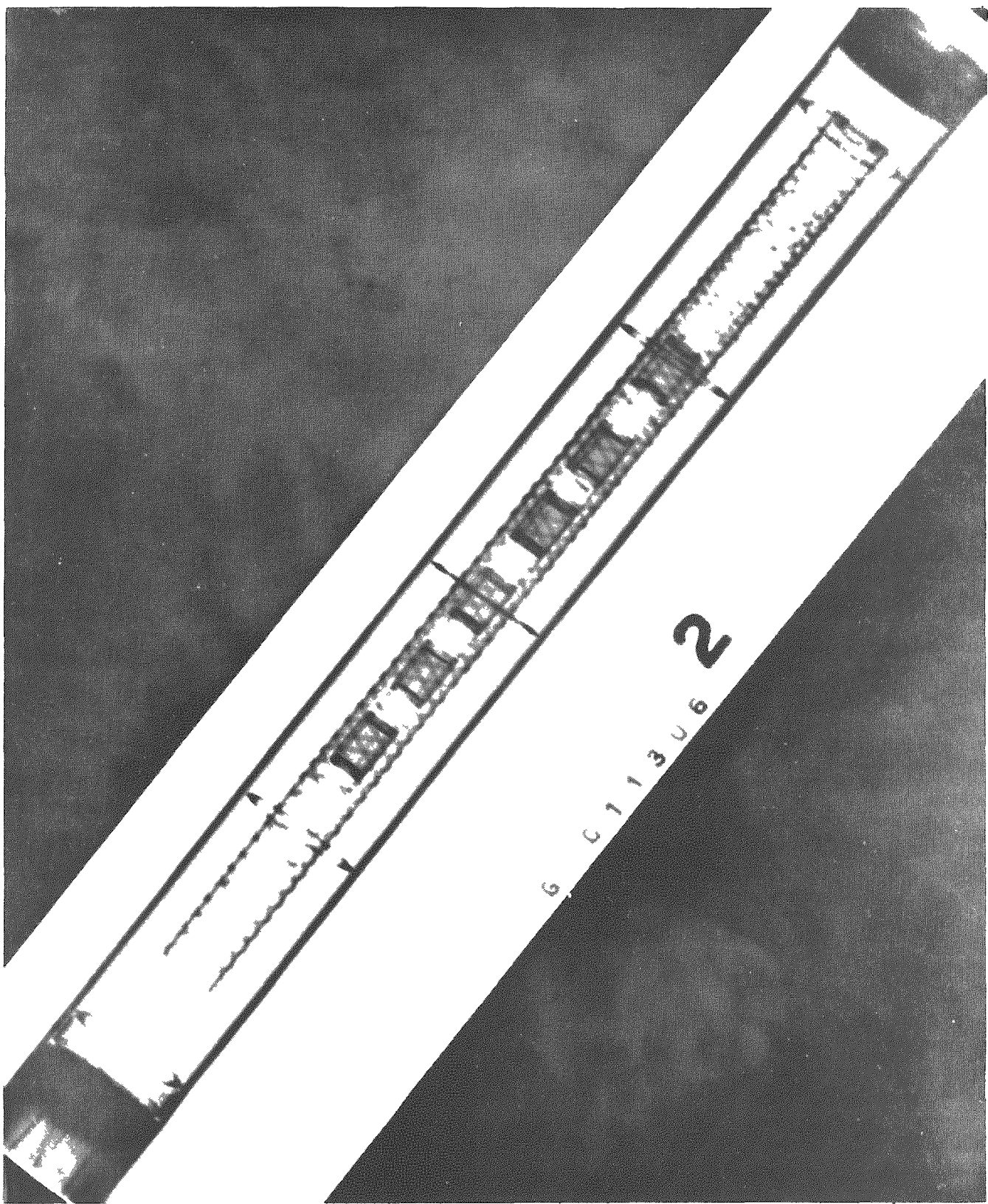


FIGURE 3. CAPSULE ASSEMBLY DETAILS



N50660

FIGURE 4. CAPSULE COMPONENTS READY FOR ASSEMBLY



N50992

FIGURE 5. RADIOGRAPH OF COMPLETED CAPSULE

furnace tube without etching through the 10-mil heater sheath. Any leak in the heater sheath, of course, will permit the high-pressure gas to escape along the length of the heater through the MgO insulation.

Four Type 304 stainless steel-sheathed MgO-insulated Chromel-Alumel thermocouples were provided to measure specimen temperatures. These were located inside the furnace tube as follows:

<u>Thermocouple</u>	<u>Recorder</u>	<u>Location</u>
P-9	1	At the side of the top specimen
Q-6	6	On the center line of the furnace tube between the third and fourth specimen from the top
P-10	11	At the side of the fourth specimen from the top
Q-10	--	At the side of the bottom specimen

The top thermocouple, P-9, was coiled and served to hold the specimen basket against a plug in the bottom of the furnace tube. All thermocouples passed between the specimens and the furnace wall. The tip of the Thermocouple Q-6 was bent inward to the center line of the furnace tube; the tips of the other couples were bent slightly inward to contact the specimens rather than the furnace wall. The thermocouple sheaths were brazed to the top end cap, and then passed through the Lavite terminal block and into the lead tube (a 1-in.-diameter stainless steel tube which was welded to the top of the capsule and extended to the top of the reactor pool), where the thermocouples were connected individually to thermocouple lead wires. A 1/8-in.-OD 1/16-in.-ID gas line from the gas-sampling system penetrated and was brazed to the top end cap.

The size of the furnace tube was dictated by the specimen size and the need to reduce end effects. It was made as small in diameter as possible to reduce the heat losses and, hence, power input. It was felt that extending the furnace tube 3 in. beyond the end specimens would reduce the end effects considerably; a longer furnace tube would have required special casking and hot-cell handling techniques. A capsule outside diameter of 1-3/4 in. was chosen to provide sufficient space between the inside capsule wall and the furnace tube for the necessary heat barriers. A larger capsule diameter would have required a heavier pressure wall, which would have increased the neutron attenuation. Also, the increased size and weight would have made postirradiation handling more difficult.

Once the limits of capsule design and dimensions were fixed by the specimen size and other considerations noted, the heat-transfer characteristics were analyzed to determine the number of heaters that would be required to hold the specimens at 1500 F. Because of the geometry of the capsule and the probability that end losses would be small compared with the radial heat loss, only the latter was considered. Neglecting the raised portions of the heaters, assuming that conduction from the heaters to the furnace tube would be sufficient to prevent appreciable axial temperature gradients between heater windings, and neglecting natural convection, the heat-transfer analysis

becomes one of determining the heat loss by radiation and conduction across the gas annulus between the 3/4-in.-OD, 13-1/2 in. long furnace tube at 1500 F and the 1-1/2-in.-ID capsule wall at about 120 F:

(1) For the radiation loss (no baffle),

$$Q_R = \sigma A_1 F_{1,2} (T_1^4 - T_2^4),$$

where

1 refers to the furnace OD

2 refers to the pressure-wall ID

$$\frac{1}{F_{1,2}} = \frac{1}{\epsilon_1} + \frac{A_1}{A_2} \left(\frac{1}{\epsilon_2} - 1 \right)$$

ϵ_1 is assumed to be 0.85

ϵ_2 is assumed to be 0.73.

$$Q_R = 1200 \text{ w.}$$

(2) For the conduction loss,

$$Q_C = \frac{2\pi k \ell (T_1 - T_2)}{\ln \frac{d_1}{d_2}},$$

where

k is assumed to be 0.034 Btu/(ft)(hr)(F) at 1000 F.

$$Q_C = 135 \text{ w.}$$

(3) For the total heat loss,

$$Q_T = Q_R + Q_C$$

$$Q_T = 1335 \text{ w.}$$

A total heat loss of 1335 w could have been handled since there was room for three 1000-w heaters on the furnace tube. However, heat loss by the natural convection of the high-pressure CO₂ was neglected in this calculation and could be expected to increase the total value somewhat. Consequently, a radiation baffle of thin Type 304 stainless sheet stock was located in the annulus between the furnace tube and outer capsule wall. This could be expected to reduce the heat loss by radiation, the major loss by about 50 per cent and reduce the total radiation and conduction loss to less than 1000 w. With 3000 w available, heater burnout or unexpectedly large convective losses could be tolerated.

The baffle had five rings fitted to its outside surface to position it concentrically with the furnace tube and to help reduce the convective flow of the gas. Other radiation baffles were placed between each end of the furnace tube and the end closures of the capsule. To reduce convective flow still further, a cap was placed over the bottom of the

furnace tube. A 1/8-in.-hole in the cap allowed some circulation since it was desirable to have all of the small quantity of CO₂, rather than just that in the furnace tube, available for reaction with the specimens.

Out-of-Pile Tests of Capsule

Before final assembly, the outer shell of the capsule was pressurized repeatedly to 3000 psi. Micrometer measurements at the critical areas, the threaded regions at the ends of the tube, indicated that the yield strength of the material had not been exceeded.

After final assembly, the capsule was operated in a tank of water to determine its heat-transfer characteristics and to obtain experience in changing the gas during operation. Argon was used in these tests to prevent premature reactions with the specimens. These tests were made with the capsule in a vertical position as it would be in a lattice position in the BRR core. It soon became evident that, despite attempts to minimize natural convection, a large temperature gradient existed along the specimen region of the furnace tube when the gas pressure was raised to 1000 psi. The gradient was a strong function of the pressure, being less than 80 F at 285 psi and 500 to 600 F at 1000 psi.

Irradiating under these conditions would have been unsatisfactory for two reasons. It would have been impossible to compare the results from different specimens because of their exposure to different temperatures. Also, the temperature at the top of the furnace tube would probably have had to be considerably higher than the 1500 F desired for the specimens, and this would have endangered the life of the heaters. Modifications to the capsule might have reduced the convective flow somewhat. However, almost any change would have involved more stainless steel in the form of baffles, which would have reduced the specimen area to capsule area still further, or the introduction of a powdered material, which might have contaminated or scavenged the gaseous environment. Because of these factors and the need to start the irradiation as promptly as possible, plans were made to operate the capsule in a horizontal position against one face of the BRR core.

The capsule was tested in a horizontal position by sealing it in a water jacket and heating the specimens to 1500 F with the furnace tube heaters as before. At 1000 psi in a horizontal position, the maximum temperature difference in the specimen region was less than 100 F. A saddle was fabricated to hold the capsule across the top of the beam tubes (about 5 in. above the horizontal center line of the core) against the face of the core. The total gamma-plus-fast-neutron dose rate in this position was estimated to be about 8×10^7 rads per hr.

Design of Associated Equipment

As mentioned previously, there were two reasons for providing facilities for gas sampling and replenishment during the irradiation. Samples taken at intervals might indicate corrosion rates and dissociation rates of the CO₂ in the radiation field. Frequent changes of the gas loading would provide a more representative reactor gas environment since the composition of the initial and perhaps subsequent loadings might be

substantially altered by reactions with the large area of capsule surface which was also at 1500 F.

The gas-sampling equipment consisted of a 25-ft length of 1/8-in. -OD 1/16-in. -ID stainless steel tube running from the capsule to the pool surface where two pressure gages, an 8-liter sampler bomb, and a tank of CO₂ were connected with small-bore copper tubing and brass valves. One pressure gage was equipped with limit switches which would scram the reactor if the pressure rose too high or ring an alarm if the pressure dropped too low. Prior to the first CO₂ loading, the system was evacuated and flushed several times with CO₂. On subsequent loadings, the system was not evacuated since at least 95 per cent of the gas was released by simply bleeding the system pressure to atmosphere pressure.

Irradiation History

The irradiation capsule was located at one face of the BRR, about 5 in. above the horizontal center line of the core as mentioned previously. The capsule and gas-sampling equipment were evacuated and flushed several times with the CO₂ that was to be used for the experiment. This was taken directly from a tank of welding-grade CO₂ with a dew point of -50 F, a negligible CO content, and a 0.024 volume per cent oxygen content. An analysis of the final purge loading gave an oxygen content of 0.06 volume per cent. Since the precision of measurement of the oxygen content in this range was probably no better than ± 50 per cent, the difference is not significant.

After the final purge, the system was pressurized to 870 psi (full tank pressure), the tank was closed off, and the capsule heaters were turned on. Because of difficulties with the heater power-supply regulation the capsule operated at only 250 F for the first day. On the second day, a temperature of 1500 was reached and maintained for about 10 hr. At that time, two of the three heaters burned out and the temperature dropped to about 1400 F. Rather than risk the remaining heater in an attempt to bring the temperature back to 1500 F (which would have required exceeding the rating of the heater) the irradiation was continued at the lower temperature.

Table 1 presents the irradiation history of the capsule. The analysis of the second gas loading indicated a high CO content. When subsequent analyses showed a decreasing CO content, it was decided to continue the irradiation at the lower temperature until the CO content reached equilibrium. After two BRR cycles (4 weeks) the CO content had dropped to about one-tenth of the highest value and it was decided to increase the temperature to 1500 F. At the higher temperature, the CO content rose again and then fell off as it had before. After a week's operation at the higher temperature, the remaining heater was still performing satisfactorily at a power level of about 1400 w - 400 w above its design rating.

Postirradiation Examination Techniques

Following the irradiation, the capsule was opened and the specimens examined in the Battelle Hot-Cell Facility. The postirradiation study included length, diameter, density, and weight determinations, metallographic examinations, and microhardness measurements. Unirradiated specimens were also examined to provide control information.

TABLE 1. IRRADIATION HISTORY AND RESULTS OF GAS ANALYSES FOR EACH CONSECUTIVE GAS LOADING

Gas Loading	Capsule Irradiation History				Gas Pressure, psi	Analysis of Gas Loading(d), volume per cent		
	Duration of Irradiation of Gas Loading(a), hr	Temperature(b), F	Time at Temperature(c), hr			Carbon Monoxide	Oxygen	
B (tank analysis)	--	--	--	--	--	Nil	0.024	
Final purge	15 sec	--	--	--	--	--	0.06	
1	29-1/2	250 1500	27-1/2 2	900 est. 900 est.	-- --	-- 0.04		
2	31-1/2	1500 1350	7-1/2 24	900 900	-- 3.6 ± 0.2	-- 0.05		
3	72-1/2	1400	72-1/2	870	3.1 ± 0.2	0.04		
4	149	1350 275 1260 275 1250	55 13 25 4 64	930 700 900 700 900	-- -- -- -- 1.1 ± 0.2	-- -- -- -- 0.4		
5	216	1275 275 1275	144 1 71	850 700 850	-- -- 0.4 ± 0.1	-- -- 0.07		
6	70 (1/2 at 1 megawatt)	1260 <200 1410 1500	67 51 1 2	900 700 930 980	-- -- -- 0.45 ± 0.15	-- -- -- 0.04		
7	99-1/2	1560 1520	21 93	1000 900	-- 1.9 ± 0.2	-- 0.07		
8	52	1500	52	1000	0.6 ± 0.2	0.06		

(a) Irradiation at 1 megawatt unless otherwise noted.

(b) Temperatures listed are for Thermocouple Q-6 in the center of the furnace. The temperatures of the end specimens were 60 to 100 F below the temperatures listed.

(c) Time periods are in order of occurrence and include reactor downtime.

(d) Approximately two-thirds of gas in sample came from the capsule; the remainder came from the external system. Unless complete mixing occurred during irradiation the absolute values for CO and oxygen in the capsule may differ from these values.

Physical Measurements

Three length measurements were made on each specimen. The measured length is the distance between the end plugs, measured weld-to-weld at 120-deg intervals. As shown in Figure 2, the weld areas are rough, and precise length measurements are difficult to make. Five diameter measurements were obtained on each specimen. Each specimen was rotated about 90 deg between measurements. Specimen densities were measured by displacement in carbon tetrachloride. The density of a standard was measured before and after each measurement on an irradiated specimen.

Metallography

Different procedures were used to prepare the irradiated and control specimens for metallographic examination.

Longitudinal and transverse sections of the control specimens were prepared for metallographic examination. Sections were mounted in plastic, and ground with water-lubricated 240-, 400-, and 600-grit silicon carbide papers. The ground specimens were polished on 240-rpm wheels using Forstmann cloth, 1- μ diamond paste abrasive, and kerosene lubrication. The Type 310 stainless steel specimens were swab etched with dilute aqua regia, and the Type 446 stainless steel specimens were etched with hydrochloric acid and ethylene glycol. The Inconel specimens were electrically etched for 5 to 15 sec in a 10 per cent oxalic acid at a potential of 6 v.

A longitudinal section of each irradiated specimen, covering about one-third the specimen length and including the end plug, was prepared for metallography. Specimens were mounted in Bakelite, ground on 240-, 400-, and 600-grit silicon carbon papers lubricated with kerosene, and polished on a Syntron vibrator using Forstmann cloth, Al₂O₃ abrasive, and water lubricant. All specimens were electrically etched by a procedure similar to that described above for the control specimens of Inconel.

Microhardness measurements were made on metallographically prepared sections of the control and irradiated specimens. A Tukon tester with a Knoop-type indenter operating with a load of 200 g was used in these determinations.

Results of Postirradiation Examination

Visual Examination

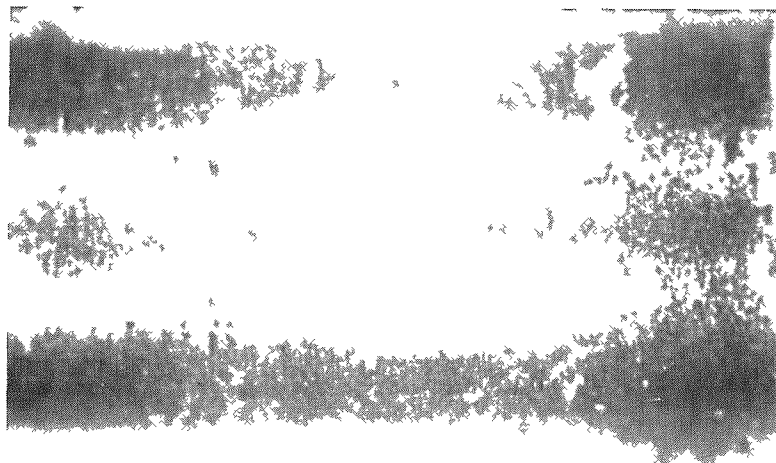
Photomacrographs of the side and end of three of the six irradiated specimens of Inconel and Types 310 and 446 stainless steel are shown in Figures 6 through 8. Photomacrographs of the other three duplicate specimens exhibit the same general appearance as those shown and are not included in the report. For comparison with the unirradiated control specimens, Figures 1 and 2 should be examined. None of the specimens showed visible evidence of swelling, cracking, or bowing, and the end plugs were all intact. All of the specimens were discolored, exhibiting a reddish-brown color characteristic of slight surface oxidation. The oxide on the welded end plugs appeared to be heavier than on the rest of the specimen. Surface irregularities observed in the control specimens were also observed in the as-irradiated specimens.



6X

HC1725

a. End View



6X

HC1726

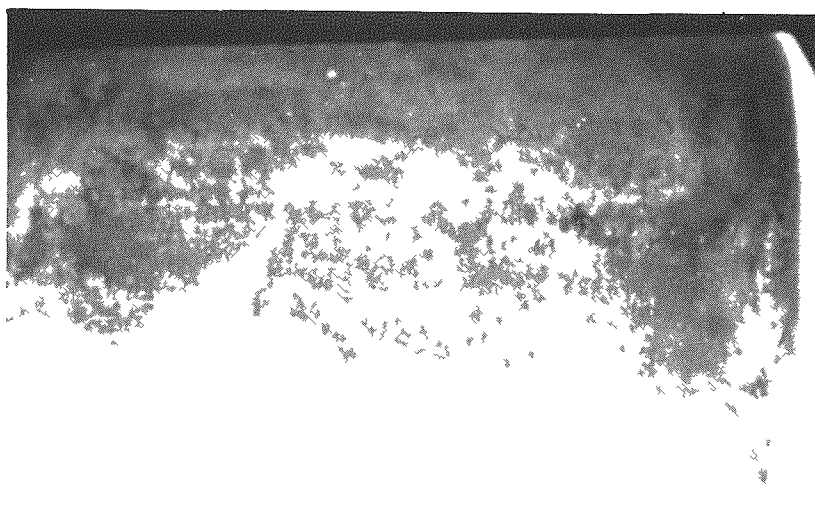
b. Side View

FIGURE 6. INCONEL SPECIMEN L-2 AFTER IRRADIATION

6X

HC1718

a. End View

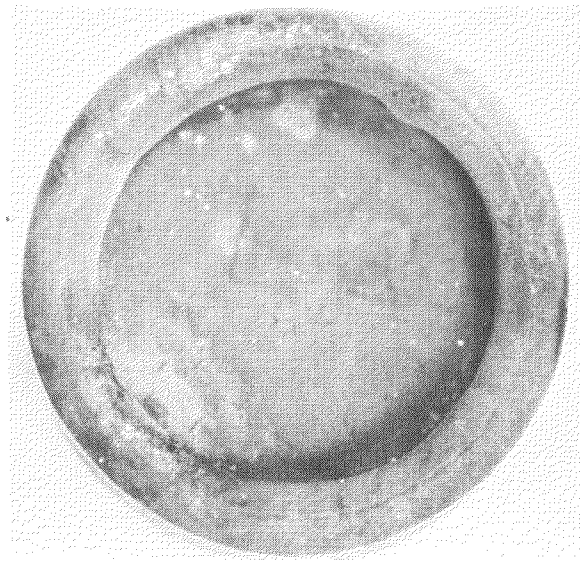


6X

HC1720

b. Side View

FIGURE 7. TYPE 310 STAINLESS STEEL SPECIMEN A-2
AFTER IRRADIATION



6X

HC1731

a. End View



6X

HC1732

b. Side View

FIGURE 8. TYPE 446 STAINLESS STEEL SPECIMEN F-3
AFTER IRRADIATION

Physical Measurements

Measurements made before and after irradiation on all six specimens are summarized in Table 2. The largest weight gains were observed in the Inconel-clad specimens. Only small changes in specimen dimensions were observed. The precision of the length measurements was poor because the welded end plugs were rough and not machined (see Figure 2). Repeated length measurements showed variations as large as 20 mils.

The length, diameter, and density values reported in Table 2 are average values based on three, five, and two measurements, respectively. Length measurements on a single specimen varied three to five units in the third decimal place while the diameter measurements varied five units in the fourth decimal place. In the density determinations the variation was about two units in the third decimal place. These precision indices should be kept in mind when the measurements in Table 2 are compared. Accordingly, the precision implied in Table 2 is considerably less than the actual precision.

The changes in length reported in Table 2 are both positive and negative and probably mean very little because of the irregular surfaces at the welded ends of the specimens. The changes in diameter, on the other hand, are consistent and probably real. They might be attributed to a buildup of an oxide film; however, neither the very small weight gains nor the metallographic examinations discussed later support this thesis.

Metallographic Examination

Microhardness measurements obtained on the cladding of the control and irradiated specimens are reported in Table 3. The hardnesses represent readings from the outer edge (gas-cladding interface) to the inner edge (cladding-graphite interface). From the metallographic results there is some evidence that decreasing amounts of carbides were present in the control specimens of Type 310 stainless, Type 446 stainless, and Inconel, in that order. These carbides make a considerable contribution to the hardness. The good control possible in the metallographic preparation of the unirradiated control specimens promotes carbide retention in the microstructure. On the other hand, remote metallographic techniques are not as easily controlled, and the loss of carbides from the microstructure of the irradiated specimens is more probable. An additional factor must also be considered when the preirradiation and postirradiation microhardness measurements are compared. At the irradiation temperature of 1500 F, fabrication stresses from the swaging operation will partially anneal out and reduce the hardness. For these reasons the microhardness measurements in Table 3 are not easily interpreted. Loss of carbide inclusions appears to explain the results given for Type 310 stainless. The hardness of the control specimen ranges from 250 to 550 DPH numbers, the higher readings occurring in the area of greatest carbide concentration. In the irradiated specimens, where carbides have been lost, the hardness is lower and much more uniform throughout the cladding.

All six irradiated specimens and the three control specimens were examined in the program. Duplicate irradiated specimens having the same cladding exhibited, in general, the same microstructure, and so a photomicrograph of only one specimen of each type is presented (Figures 9 through 11).

TABLE 2. PHYSICAL MEASUREMENTS OF SPECIMENS BEFORE AND AFTER IRRADIATION

	Specimens Clad With Inconel		Specimens Clad With Type 310 Stainless		Specimens Clad With Type 446 Stainless	
	L-2	L-7	A-1	A-2	F-1	F-3
Weight, g						
Before	8.2106	8.1302	7.2664	7.1685	7.1975	6.9226
After	8.2194	8.1463	7.2699	7.1708	7.2032	6.9238
Change	+0.0088	+0.0161	+0.0035	+0.0023	+0.0057	+0.0012
Weight Change, per cent	+0.107	+0.198	+0.048	+0.032	+0.079	+0.017
Density, g per cm ³						
Before	5.09	4.88	4.39	4.39	4.72	4.56
After	5.10	4.87	4.40	4.41	4.66	4.56
Change	+0.01	-0.01	+0.01	+0.02	-0.06	--
Density Change, per cent	+0.2	-0.2	+0.2	+0.5	-0.3	--
Length, in.						
Before	0.709	0.732	0.716	0.706	0.703	0.704
After	0.700	0.729	0.706	0.700	0.712	0.713
Change	-0.009	-0.003	-0.010	-0.006	+0.009	+0.009
Length Change, per cent	-1.2	-0.5	-1.3	-0.8	+1.3	+1.2
Diameter, in.						
Before	0.4401	0.4400	0.4481	0.4475	0.4409	0.4412
After	0.4448	0.4423	0.4501	0.4493	0.4482	0.4508
Change	+0.0047	+0.0023	+0.0020	+0.0018	0.0073	+0.0096
Diameter Change, per cent	+1.0	+0.5	+0.5	+0.4	+1.7	+2.2

TABLE 3. MICROHARDNESS MEASUREMENTS OF
SPECIMEN CLADDINGS

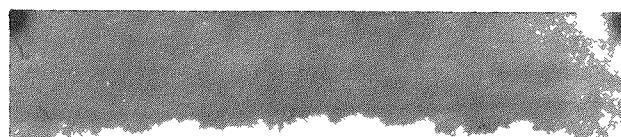
Specimen	Knoop Hardness From Gas-Cladding to Cladding-Graphite Interfaces									
	<u>Inconel Cladding</u>									
L-3 (control)	252	338	327	327	325	327	327	322	335	317
L-2	177	191	197	207	220	203	217	231	224	183
L-7	142	171	179	186	174	174	154	174	176	169
<u>Type 310 Stainless Steel Cladding</u>										
A-3 (control)	266	257	302	274	270	355	380	492	549	
A-1	188	222	231	233	256	217	240	263		
A-2	185	213	211	208	207	207	201	185		
<u>Type 446 Stainless Steel Cladding</u>										
F-2 (control)	202	230	261	284	276	302	261	280	254	
F-1	215	240	224	229	240	228	224	231	236	220
F-3	162	192	183	208	186	181	161	191	194	181



250X

RM11041

a. Outer or Gas-Metal Interface
of Control Specimen L-3



250X

HC1900

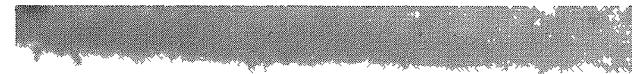
b. Reaction at Gas-Metal Interface
of Specimen L-2 After Irradiation



250X

RM11040

c. Inner or Graphite-Metal Interface of
Control Specimen L-3

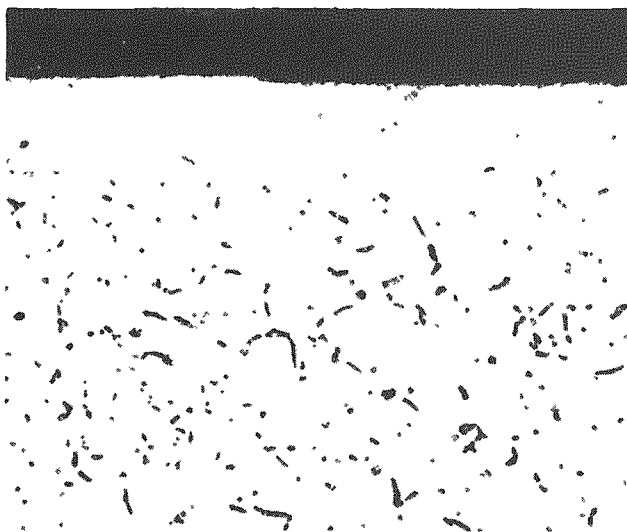


250X

HC1903

d. Inner or Graphite-Metal Interface
of Specimen L-2 After Irradiation

FIGURE 9. INCONEL MICROSTRUCTURES AT THE GAS-CLADDING AND
CLADDING-GRAPHITE INTERFACES OF CONTROL
SPECIMEN L-3 AND IRRADIATED SPECIMEN L-2



250X

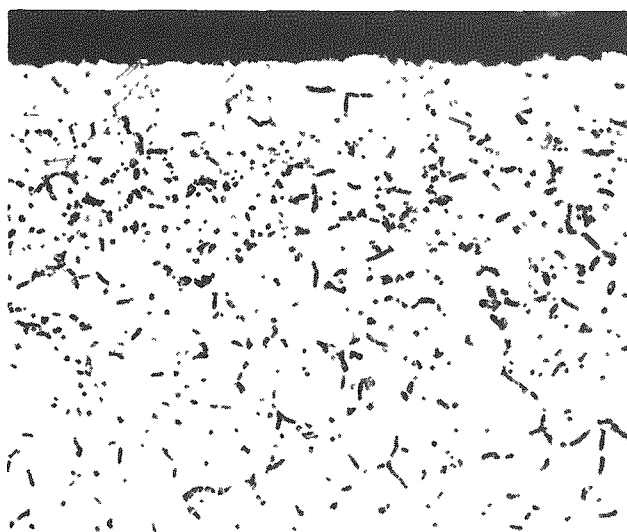
RM11023

a. Outer or Gas-Metal Interface
of Control Specimen A-3

250X

HC1896

b. Gas-Metal Reaction at Interface
of Specimen A-2 After Irradiation



250X

RM11031

250X

HC1895

c. Inner or Graphite-Metal Interface
of Control Specimen A-3

d. Inner or Graphite Metal Interface
of Specimen A-2 After Irradiation

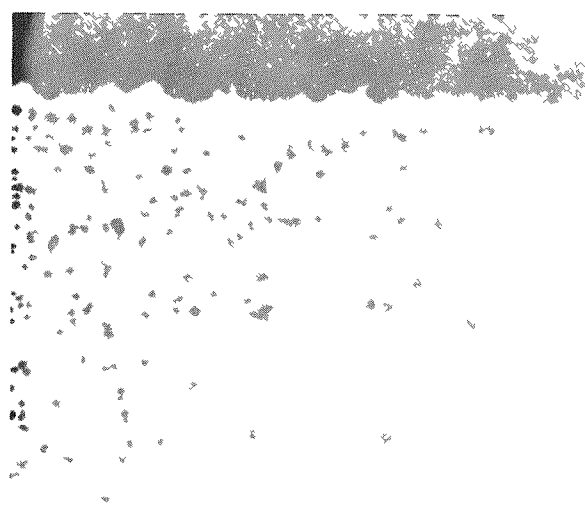
FIGURE 10. TYPE 310 STAINLESS STEEL MICROSTRUCTURES AT
GAS-CLADDING AND CLADDING-GRAPHITE
INTERFACES OF CONTROL SPECIMEN A-3 AND
IRRADIATED SPECIMEN A-2



250X

RM11044

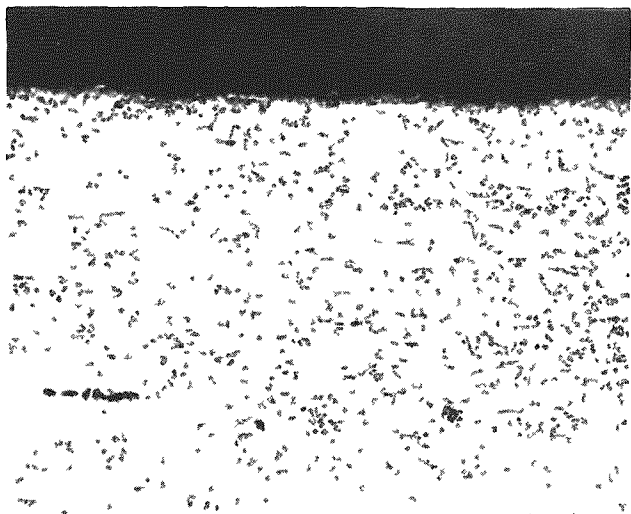
a. Outer or Gas-Metal Interface of Control Specimen F-2



250X

HC1898

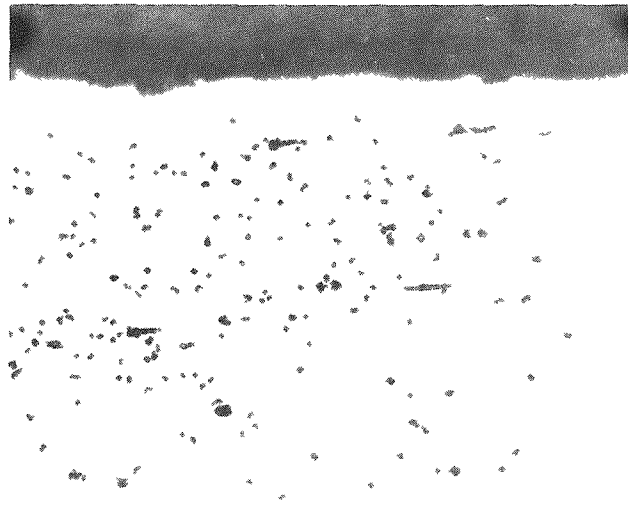
b. Reaction at Gas-Metal Interface of Specimen F-3 After Irradiation



250X

RM11043

c. Inner or Graphite-Metal Interface of Control Specimen F-2



250X

HC1897

d. Inner or Graphite-Metal Interface of Specimen F-3 After Irradiation

FIGURE 11. TYPE 446 STAINLESS STEEL MICROSTRUCTURES AT GAS-CLADDING AND CLADDING-GRAPHITE INTERFACES OF CONTROL SPECIMEN F-2 AND IRRADIATED SPECIMEN F-3

The fields of view in the photomicrographs discussed below include 8 to 10 mils of the cladding. The minimum area that can easily be distinguished in the photomicrographs is perhaps 1/16 in. wide, and equivalent to about 0.25 mil.

Inconel. The postirradiation microstructure of the gas-metal interface Specimen L-2 is shown in Figure 9b. Comparison of Figures 9a and 9b shows a marked decrease, in grain size (and also in microhardness, see Table 3) of the irradiated specimen, indicating that the Inconel cladding has undergone recrystallization during the in-pile experiment. Traces of preirradiation grain boundaries are also evident.

In addition to recrystallization and softening, it is apparent that some corrosion by CO_2 has occurred at the gas-metal interface. Small patches of oxide can be observed in areas along the metal surface, and the surface is roughened and irregular, in contrast to the control specimen, L-3. There is some evidence of intergranular corrosion.

Microstructures of the metal-graphite interfaces are compared in Figures 9c and 9d. There is no evidence of graphite-Inconel incompatibility nor surface roughening or carburization of the Inconel cladding.

Type 310 Stainless Steel. Microstructures of the gas-metal interfaces of control and irradiated specimens are shown in Figures 10a and 10b, respectively. The surface of the control specimen is smooth, while the irradiated specimen is rough and shows evidence of corrosion by the coolant gas. A narrow band with little structure may be observed along the surface (Figure 10b). This band can also be observed in the metal-graphite surface (Figure 10a). The bands were first noticed during examination of the control specimens and appeared to be associated with decarburized zones occurring in the gas-metal and metal-graphite surfaces. Figures 10a and 10c show voids produced by etching of carbide precipitates. The voids are sparse at the gas-metal surface, becoming thicker toward the metal-graphite interface until they approach the narrow band mentioned above. The presence of a carbide gradient in the control specimens is also suggested by the hardness data for the Type 310 stainless control specimen reported in Table 3.

Grain size remained unchanged in the irradiated specimen, although twinning occurred in excess of that observed in the control. The cladding appears to be compatible with graphite under the conditions of the irradiation experiment.

Type 446 Stainless Steel. Gas-metal interfaces of the control and irradiated specimens are shown in Figures 11a and 11b. As observed for both the Inconel and the Type 310 stainless specimens, the cladding surface of the irradiated specimen was rough, indicating some corrosion by the CO_2 . The specimen in Figure 11b was etched heavily to bring out grain boundaries, and the etchant attacked the precipitates and produced voids.

Microstructures of the graphite-metal interfaces of control and irradiated specimens are shown in Figures 11c and 11d, respectively. The absence of precipitates at the graphite-metal interface of the irradiated specimen may indicate some reaction of the metal with graphite, although the amount of reaction was certainly small.

Irradiation has no apparent effect on the grain size of the Type 446 stainless, although the lower hardness of the irradiated specimens (see Table 3) may indicate some annealing of work stresses in the cladding.

CONCLUSIONS

Specimens of AGOT graphite fully clad with Type 310 stainless, Type 446 stainless, or Inconel were irradiated for 5 weeks in the BRR in 1000-psi CO₂ at temperatures of 1200 to 1500 F. The purpose of this single-capsule experiment was to study the effect of the radiation-temperature-CO₂ environment on the cladding, and the graphite-cladding reaction.

Small changes in density, dimensions, and weight were observed, but only the latter may be significant. During the in-pile period samples of the capsule gas were analyzed for CO and oxygen. Compared with the initial gas charged to the capsule, no significant change in oxygen concentration was observed, but the CO increased from zero concentration to values as high as 3.6 volume per cent. The CO concentration depended on capsule temperature.

All the cladding materials had undergone some oxidation, as evidenced by specimen discoloration, and the surface roughening and small depth of attack observed in photomicrographs at 250X. The depths of attack were less than 1 mil, if oxide spalling is neglected. None of the specimens showed evidence of carburization at the graphite-metal interface. Changes in the microstructure and the microhardness of the cladding materials were observed. Recrystallization and annealing of cold-worked structures present in the as-received specimens were responsible for some of these changes.

Until out-of-pile data on duplicate specimens can be compared with the results of the irradiation experiment there is no evidence that radiation enhances the CO₂-metal or graphite-metal reactions.

REFERENCES

- (1) McIntosh, A. B., and Bagley, K. G., "Selection of Canning Materials for Reactors Cooled by Sodium/Potassium and CO₂", *J. Inst. Metals*, 84, 251 (March, 1956).
- (2) Harteck, P., and Dondes, S., "Decomposition of CO₂ by Ionizing Radiation, Part II", *J. Chem. Phys.*, 26 (6), 1727 (1957).
- (3) Cockcroft, J., "The Further Developments of the United Kingdom Nuclear Power Programme", *Nuclear Engineering*, 3 (25), 176 (April, 1958).